N89-22953

FINITE ELEMENT ANALYSIS OF A MICROMECHANICAL DEFORMABLE MIRROR DEVICE

T. J. SHEERER, W. E. NELSON AND L. J. HORNBECK
TEXAS INSTRUMENTS INCORPORATED, DALLAS TX.

ABSTRACT:

Texas Instruments has developed a monolithic spatial light modulator chip consisting of a large number of micrometer-scale mirror cells which can be rotated through an angle by application of an electrostatic field. The field is generated by electronics integral to the chip. The chip has application in photoreceptor based non-impact printing technologies. Chips containing over 16000 cells have been fabricated, and have been tested to several billions of cycles. Finite Element Analysis (FEA) of the device has been used to model both the electrical and mechanical characteristics.

INTRODUCTION:

The very high component density achieved in integrated circuits is well-known. Using the same processing techniques it is also possible to produce micromechanisms on a similar scale. Petersen (1) has described the manufacture and testing of extremely small silicon cantilevers and also lists several commercial applications of micromechanical devices.
The deformable mirror device (DMD) consists of a chip containing a large number of mirror cells as shown in Fig.(1). The cell consists of a 19um x 19 um aluminum mirror pivoted at two corners by 4.5 um beams. The mirror and its support structure are 0.375um in thickness while the beam is of nominal width 1.0 um and nominal thickness 0.08 um. 2.3 um below the structure are two address electrodes and two landing electrodes. To rotate the mirror through an angle, , a bias potential, ϕ_b, is applied to the upper structure and landing electrodes while appropriate address potentials are applied to the address electrodes as shown in Fig.(2). The cell may be used as an optical lever to deflect a light beam in and out of the field of a projection lens as shown in Fig.(3). The effect is thus of being able to activate and deactivate a "pixel" at the very high speed of the DMD cell. The DMD is more fully described in (2) and (3). In an electronic printer using a xerographic type process the light is used to selectively dissipate charge on a transfer medium, prior to the charge being transfered to paper, allowing the selective deposition of "toner" material on the paper. The most common type of printer using this process is the laser printer, which requires in addition to the laser a complex optical system and a mechanically rotating mirror to 'scan' the transfer medium. Use of the DMD (Fig.(4)) is simpler, allowing use of a conventional

incandescent source. Additionally, by variation of the "on" time of the cell, the DMD allows use of grey-scale printing. Mechanical analysis of such devices by FEA is not different from analysis of large structures, the only requirement being judicious choice of units for dimensions and mechanical properties to avoid faults due to arithmetic overflow or underflow. Electrostatic analysis is also relatively simple, as the equations of electrostatics are identical with those of heat transfer. By use of COSMIC NASTRAN in these applications it is possible to accurately model the behavior of a DMD and assess the effects of design modifications without the very considerable expense of a production run.

EQUATIONS OF ELECTROSTATICS AND THEIR ANALOGS:

The analogy between electrostatics and steady-state heat transfer is exact, and NASTRAN's heat transfer capabilities can be used in the solution of electrostatic field problems without modification. In heat transfer we have:

$$\dot{q} = - k . \nabla T \qquad (1)$$

whereas in electrostatics the polarization, D*, is given by:*

$$D = - \varepsilon . \nabla V \qquad (2)$$

Heat sources and sinks are equivalent to point charges and fixed temperatures are equivalent to fixed potentials. In electrostatics the potential gradient is refered to as the field, E*. There is no directly analogous term in heat transfer. The analogy between the different terms is listed in Table (1) below:*

TABLE 1: ANALOGY BETWEEN ELECTROSTATICS AND HEAT TRANSFER

HEAT TRANSFER	ELECTROSTATICS
TEMPERATURE	POTENTIAL V
TEMPERATURE GRADIENT	ELECTRIC FIELD E
HEAT FLUX	POLARIZATION D
HEAT SOURCE	POINT CHARGE q
CONDUCTIVITY	PERMITTIVITY ε

The force exerted on a charge by an electric field is given by:

$$\boldsymbol{F} = q \cdot \boldsymbol{D} \qquad (3)$$

where **D** is the electric polarization and q the charge. As the charge itself contributes to the field it is necessary to integrate the above expression to obtain a useful expression in terms of **E**, giving normalized force, or pressure, in vacuo:

$$\boldsymbol{F} = 0.5\, \varepsilon_0 \boldsymbol{E}.\boldsymbol{E} \qquad (4)$$

where is the permittivity of free space. This expression allows calculation of the pressure exerted at an element face directly from the output of the finite element analysis. The charge distribution resulting from a potential distribution is obtainable from the single point constraint forces which in the case of heat transfer indicate heat sources and sinks. One important difference in behaviour between the electrostatic case and the thermal case is that a conducting material acts in electrostatics in a manner equivalent to an infinitely conductive material in heat transfer, so that all points on the conductor are at the same potential. This can be modelled by appropriate constraints in the NASTRAN input deck.

ELECTROSTATIC MODEL OF THE DMD:

A 3-D model of the DMD cell was constructed using solid elements as shown in Fig.(5). Fig.(6) plots the z-component of the electric field ,**E**z, vs. x-coordinate at the center and edge of the model for a bias potential of -12V and address potentials of +5V and zero. Fig.(7) is a fringe plot of **E**z superimposed on the model. On the basis of the results obtained it was determined that fringeing effects were of relatively small significance and a series of 2-D models were made with mirror rotation angles form 1 to 9 degrees in the XY plane. Rotation of approximately 9.2 degrees was sufficient to bring the mirror in contact with the landing electrode. From each of these models The useful component of electric field, **E**y, was obtained as a function of location on the mirror. In increments corresponding to element size on the model, the force exerted on the mirror was calculated as a function of location using **E**y and the mirror's width as a function of location.Figs.(8-11) are fringe plots of potential V and field **E**y for two different rotation angles, Figs.(12-13) plot **E**y vs. location for different rotation angles for bias potentials of -12V and -16V, with an address potential of +5V. The choice of +5V allows use of standard (TTL or CMOS) logic electronics to control the DMD, with the bias potential being generated separately.

MECHANICAL MODEL OF THE DMD:

The mechanical model of the DMD was constructed in order to verify the assumption that the device acted as a rigid body (the mirror) mounted on torsion rods. Using the measured dimensions of the device a model was constructed using plate and bar elements and subject to modal and static analysis. It was determined that deformation of the mirror plate was negligible, and that the torsion bars had three deformation modes of interest with frequencies of 56.2, 192 and 545 kHz. as plotted in Fig.(14). The higher modes involved plate deformation at very high frequencies. These results indicated that the elastic constants used were valid (experimentally the first mode was at approximately 54 kHz) and that in applying electrostatic forces to the mirror it was valid to use a single lumped force at an arbitrary node, and not necessary to apply pressures over each element of the DMD model. It was also determined from this model that a force of 1.74 millidynes applied at the DMD tip was required to fully rotated the mirror.

RECONCILIATION OF MODELS AND EXPERIMENTAL DATA:

Using the electrostatic DMD model it is possible to plot force or torque on the DMD against angle for different bias and address potentials. It should be possible to predict the potentials at which the device can fully rotate. In this circumstance the electrostatic force will exceed the mechanical restoring force at all angles of rotation, and will tangentially approach the restoring force curve at a critical angle which is readily determined experimentally. Experimentally, for an address potential of 5V, a bias potential of -16V is found necessary, with a critical angle around 5.5 degrees. Fig.(15) shows experimental data plotting bias voltage vs. address voltage for spontaneous rotation. Fig.(16) plots the net force on the DMD from electrostatic fields vs. angle for an address potential of +5V and bias potential of -12V and -16V. Also plotted is the mechanical restoring force based on the finite element structural model of the DMD. The curve for -16V does appear to tangentially approach the mechanical force curve at around 5 degrees, and thus is in excellent agreement with the experimental data.

CONCLUSIONS:

The use of very simple 2-D models of electrostatic fields has proven to give accurate values of electrostatic forces in a micromechanical device. It appears likely that any desired accuracy is attainable if a sufficiently complex model is used. The response time of the device, although fast for a mechanism, is much less than the rise time of the electrode potentials. Thus the data on force vs. rotation could also be used in a transfer function or nonlinear spring input to allow dynamic modelling of the device.

REFERENCES:

*(1) Kurt E. Petersen, "Silicon as a Mechanical Material", Proc. IEEE, **70-5**, 420, (1982)*

*(2) L.J. Hornbeck, "128x128 Deformable Mirror Device", IEEE Trans. Electron Devices **ED-30(5)**, 539, (1983)*

*(3) D.R. Pape and L.J. Hornbeck, "Characteristics of the Deformable Mirror Device for Optical Information Processing", Optical Engineering, **22(6)**, 675 (1983)*

FIG. (1)

BISTABLE DEFORMABLE MIRROR DEVICE

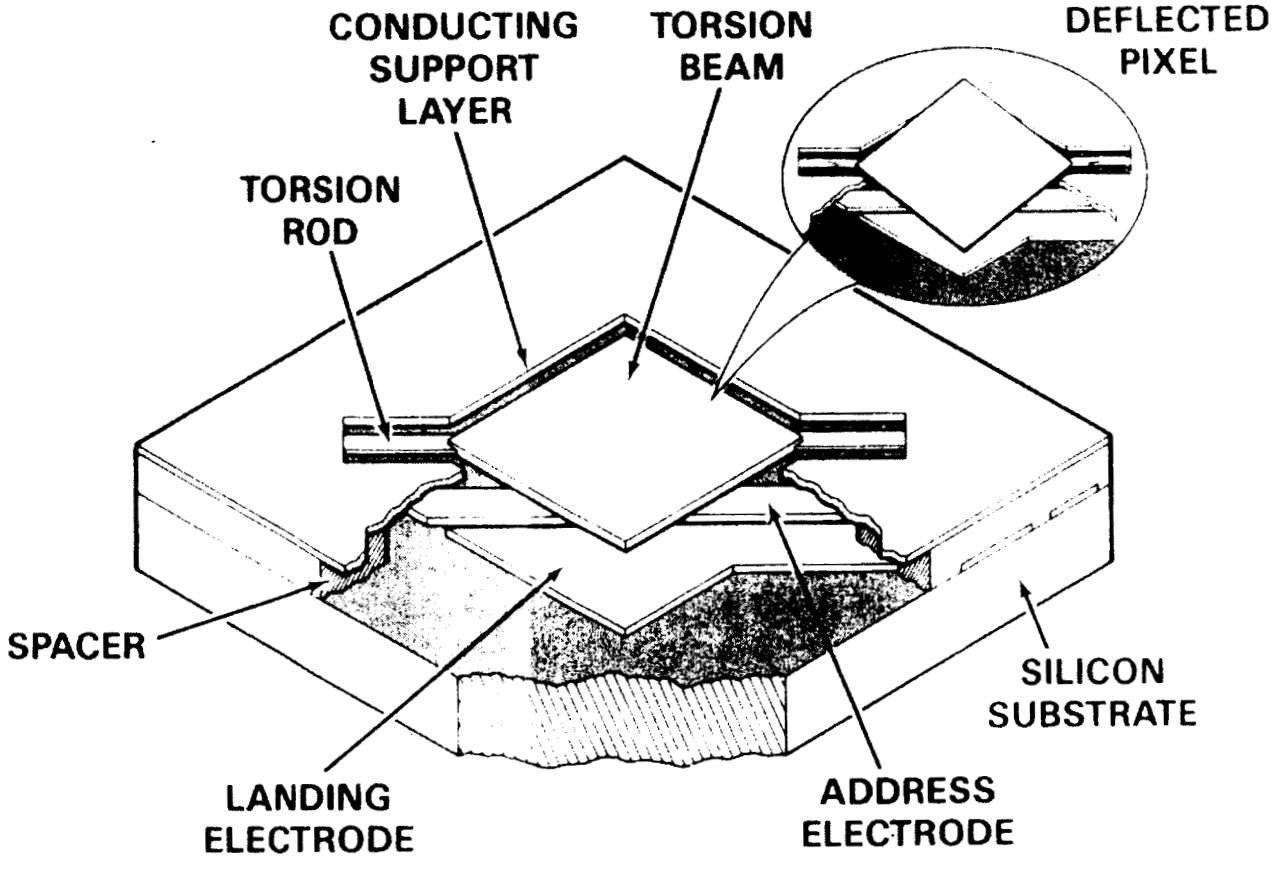

FIG. (2)

BISTABLE DMD
SCHEMATIC CROSS SECTION

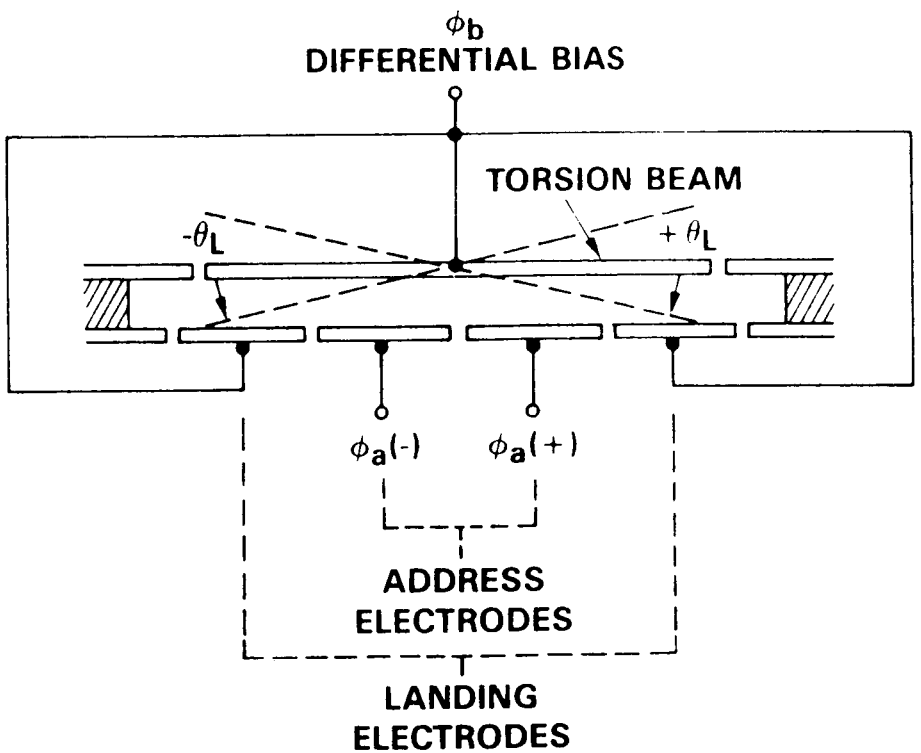

FIG. (3)

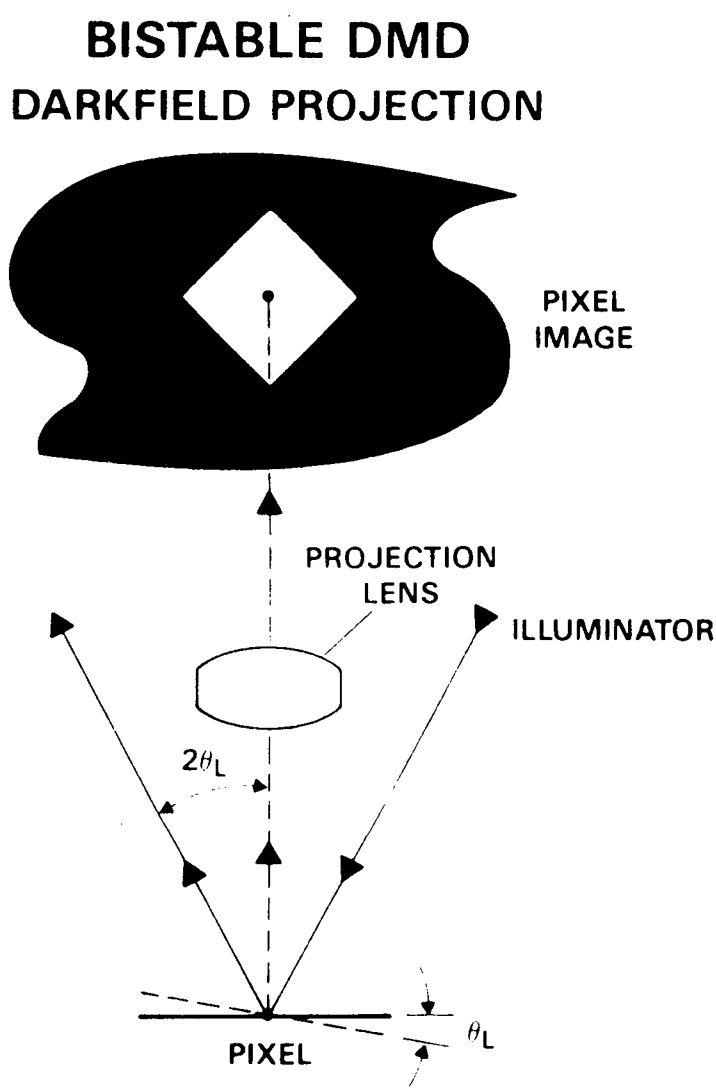
BISTABLE DMD
DARKFIELD PROJECTION
PIXEL
IMAGE
PROJECTION
LENS
ILLUMINATOR
$2\theta_L$
θ_L
PIXEL

FIG.(4)

DMD LIGHT MODULATOR SYSTEM WITH PRINTER

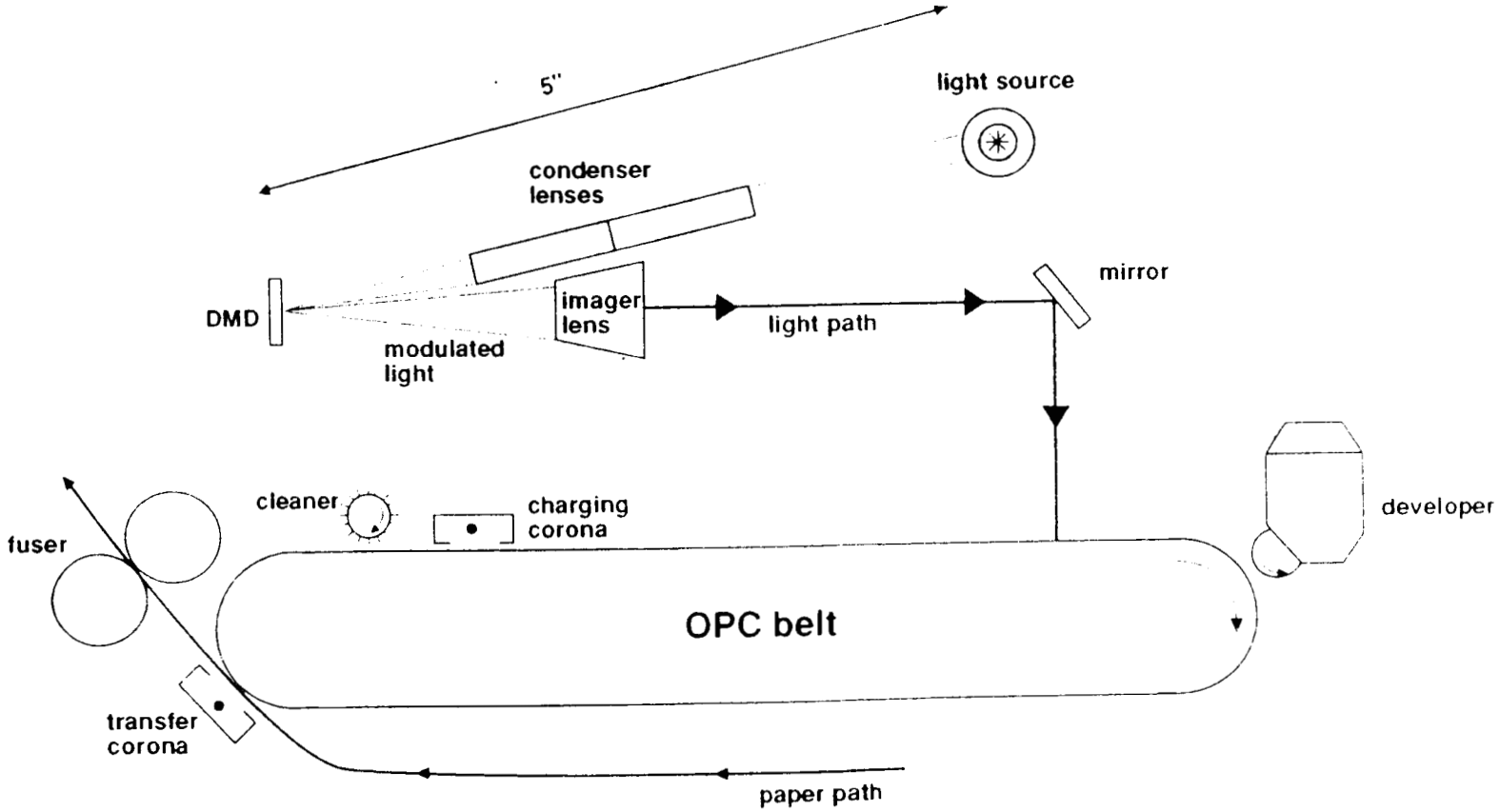

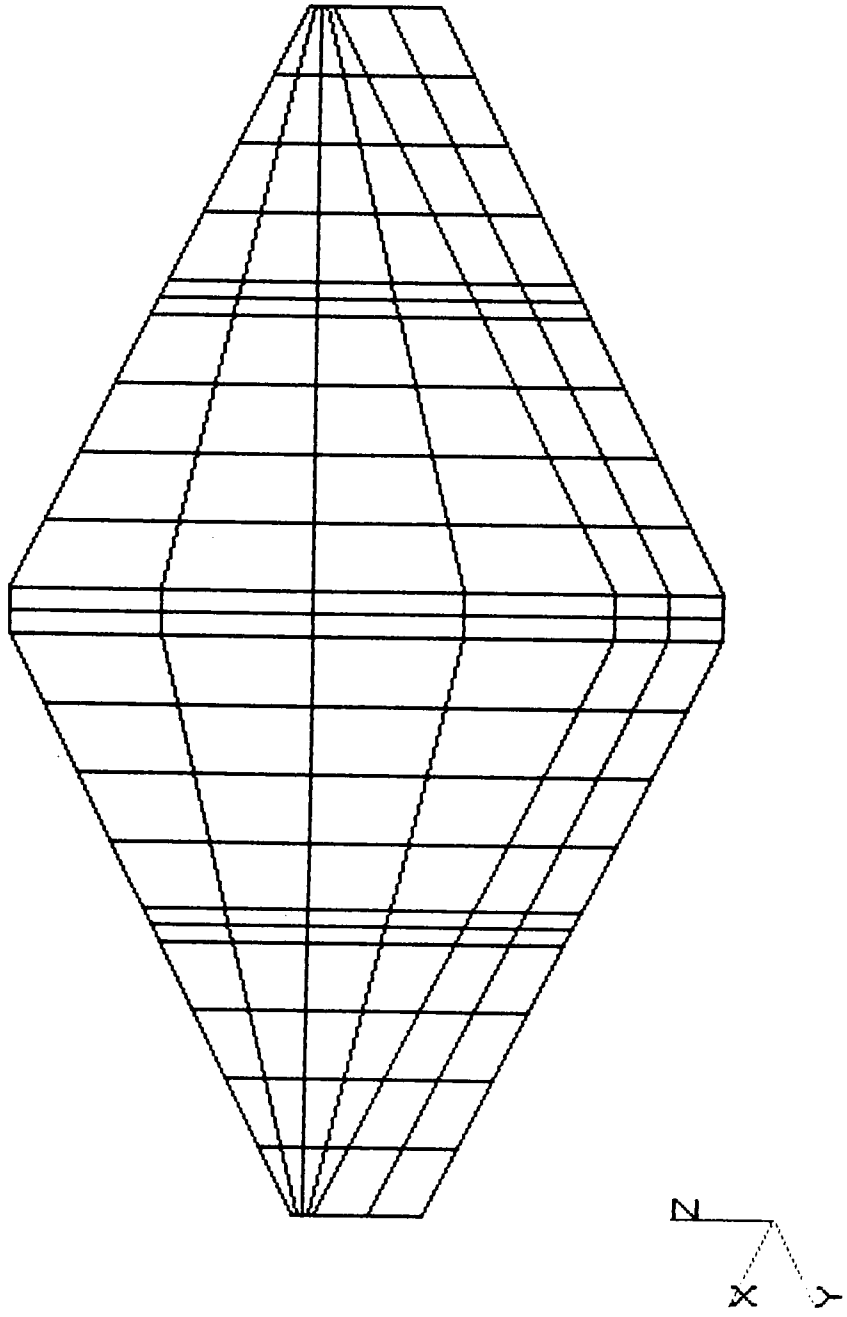

FIG.(5), 3-D MODEL OF DMD

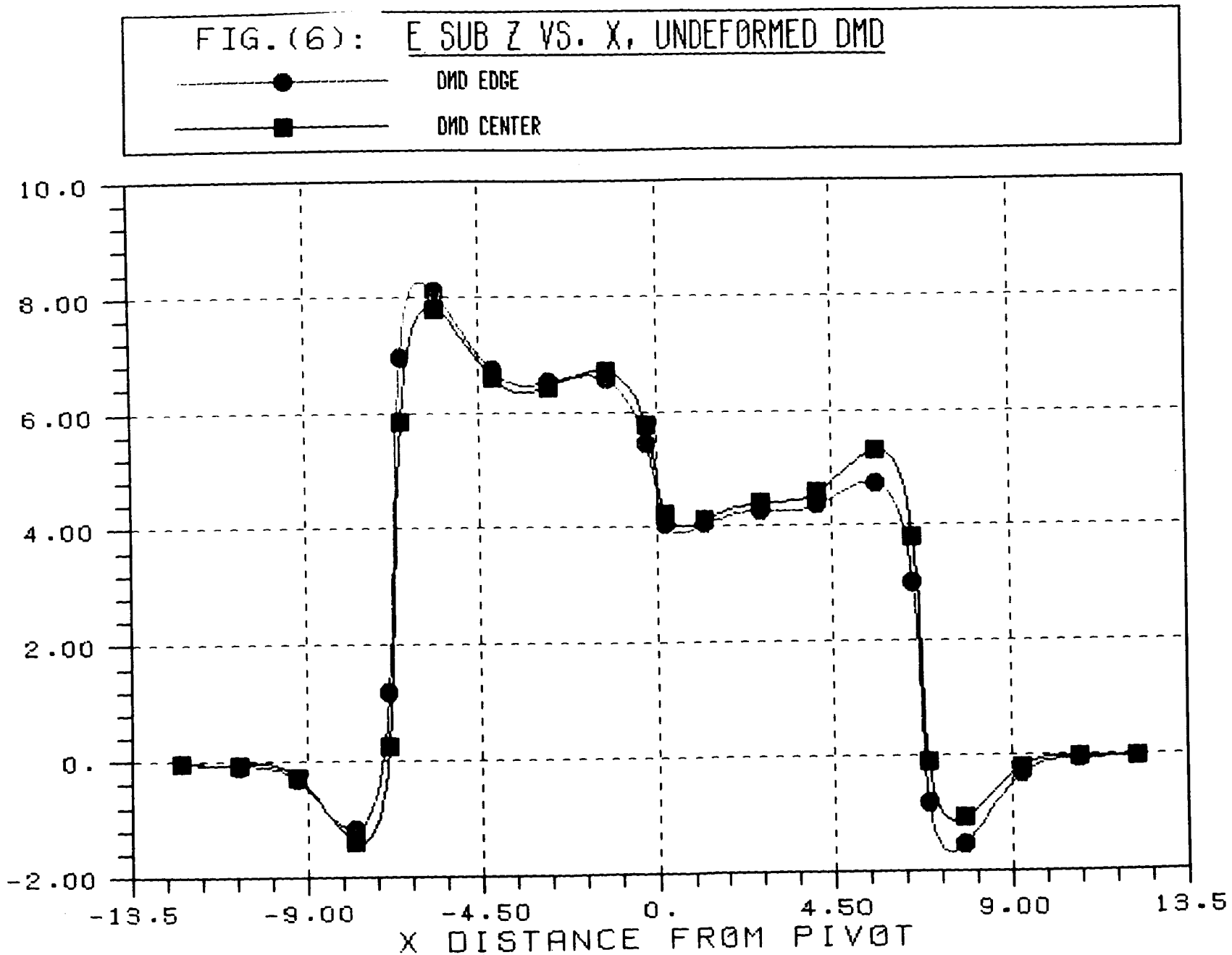
FIG.(6): E SUB Z VS. X, UNDEFORMED DMD
DMD EDGE
DMD CENTER
10.0
8.00
6.00
4.00
2.00
0.
-2.00
-13.5
-9.00
-4.50
0.
4.50
9.00
13.5
X DISTANCE FROM PIVOT

FIG(7), E SUB Z IN 3-D MODEL OF DMD

FIG.(8): POTENTIAL PLOT, DMD AT 3 DEGREES

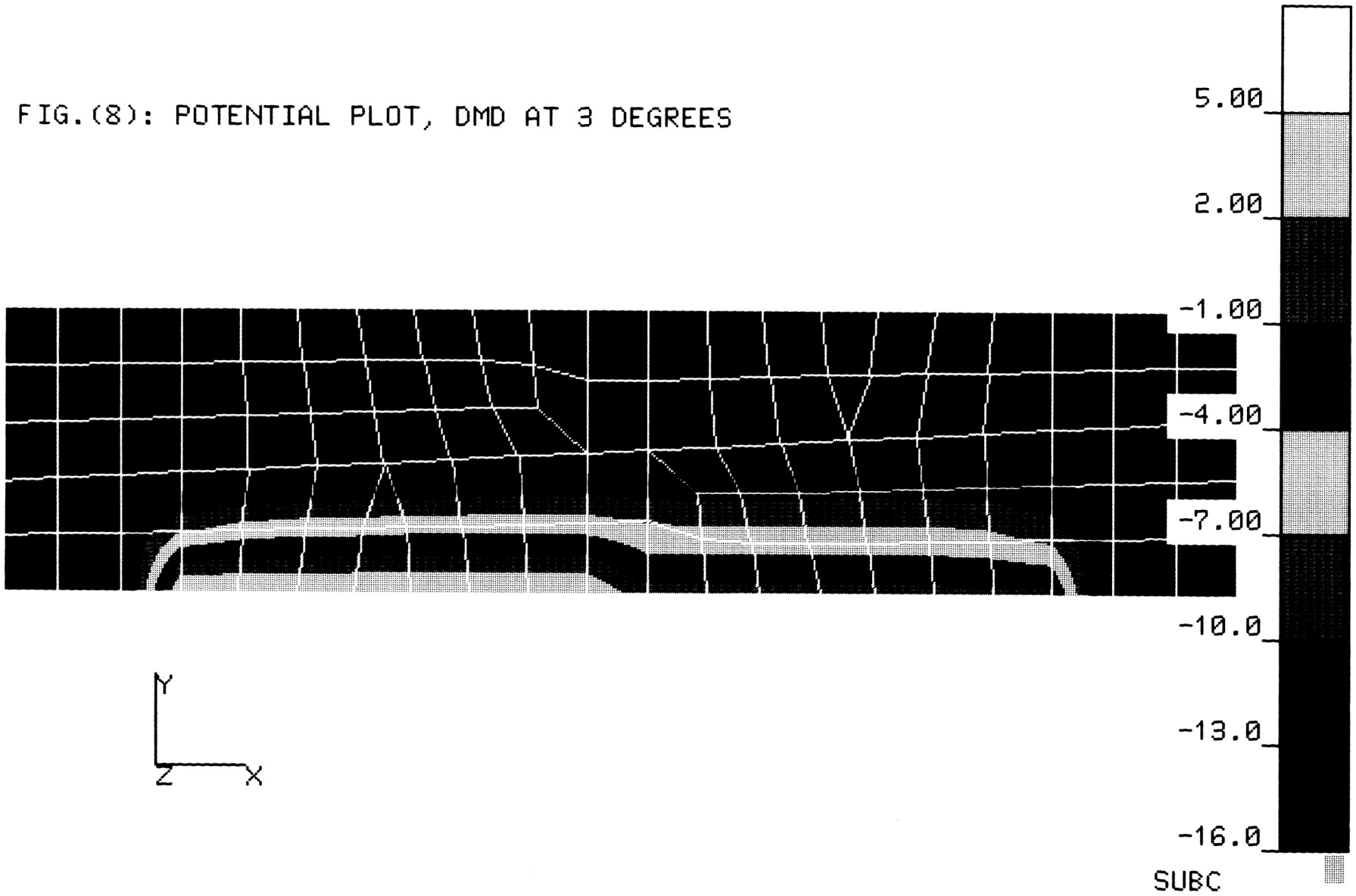

FIG(9), E SUB Y, DMD AT 3 DEGREES

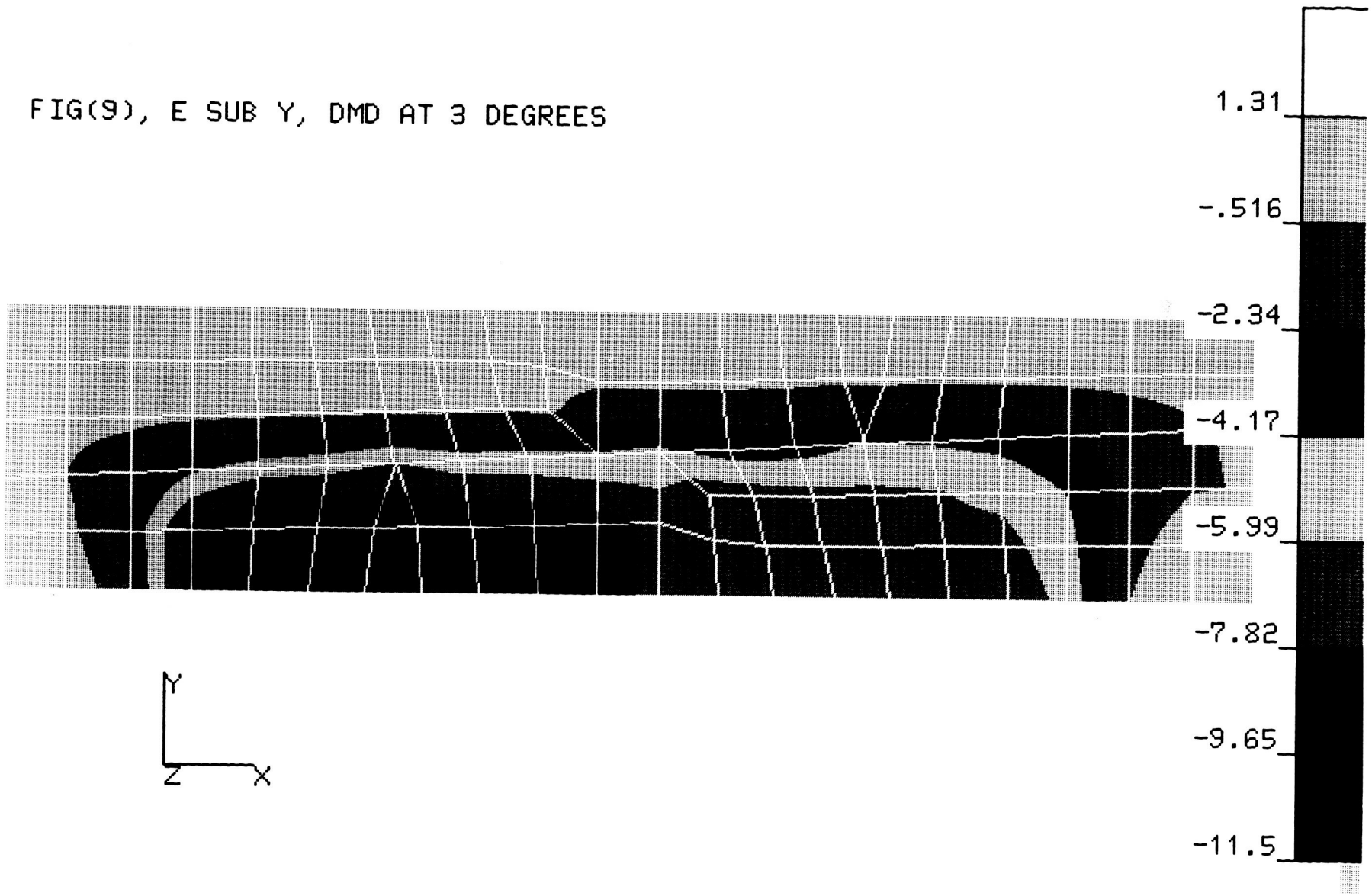

FIG.(10):, POTENTIAL PLOT, DMD AT 9 DEGREES

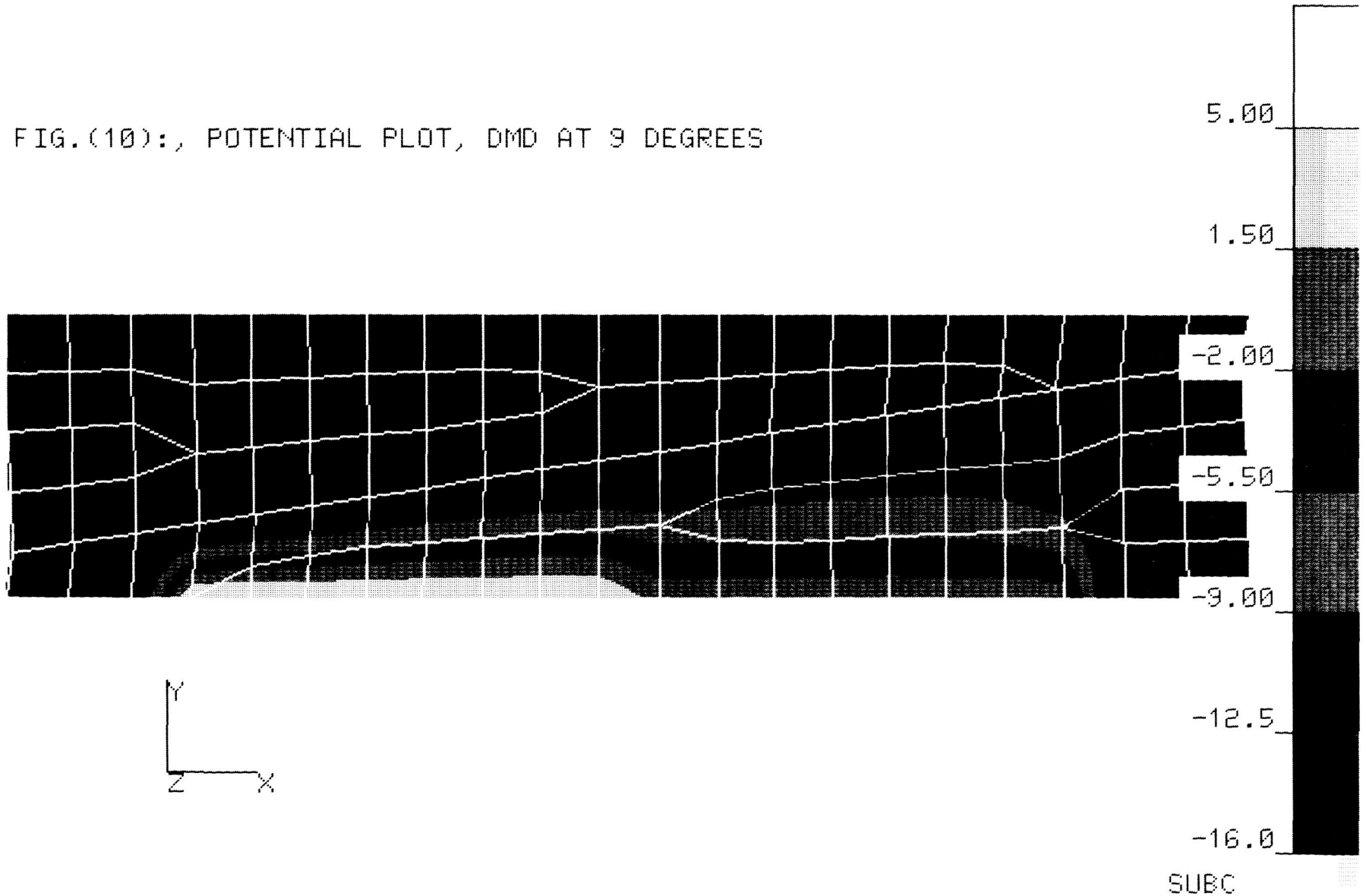

FIG(11): E SUB Y, DMD AT 9 DEGREES

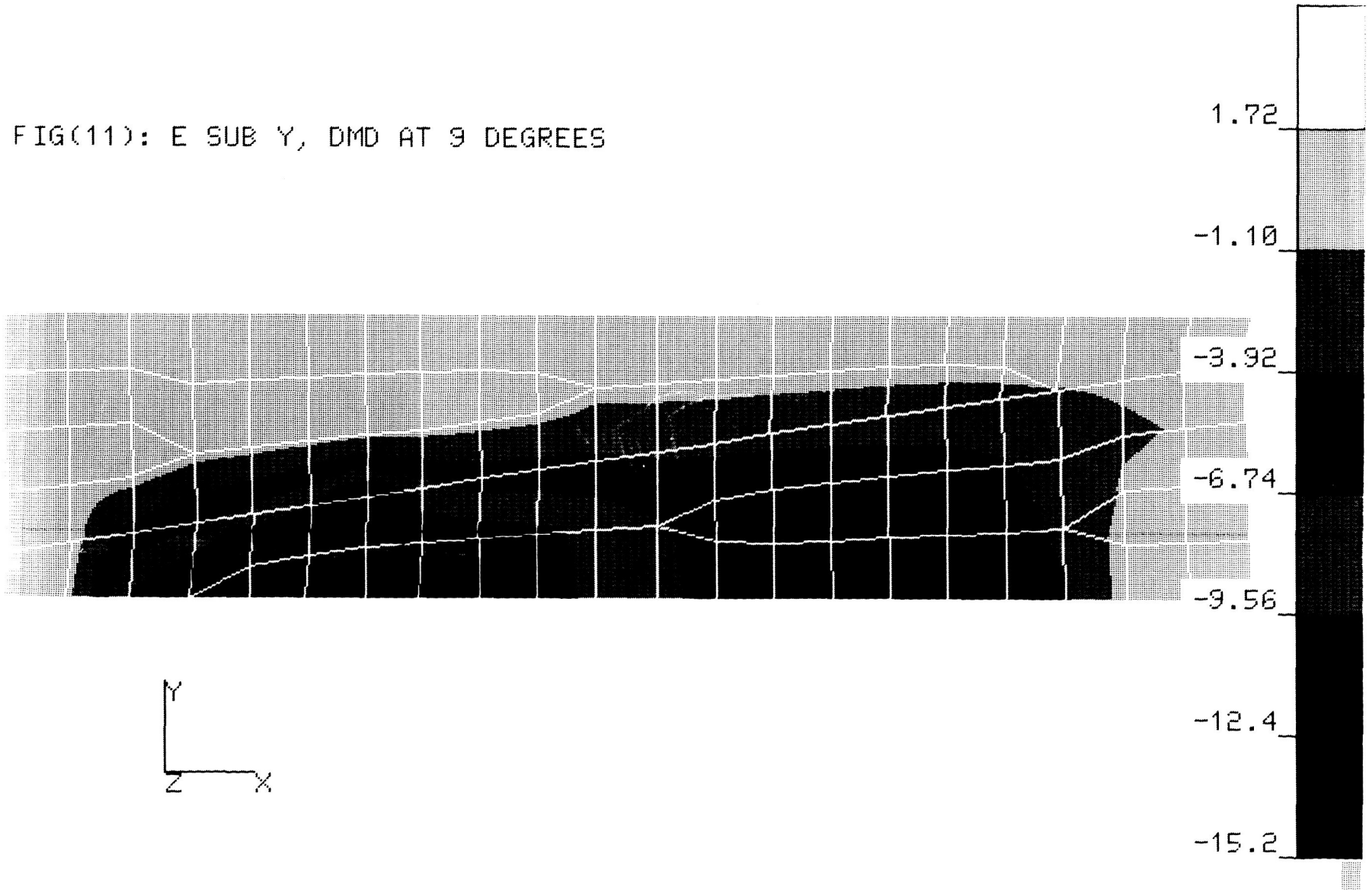

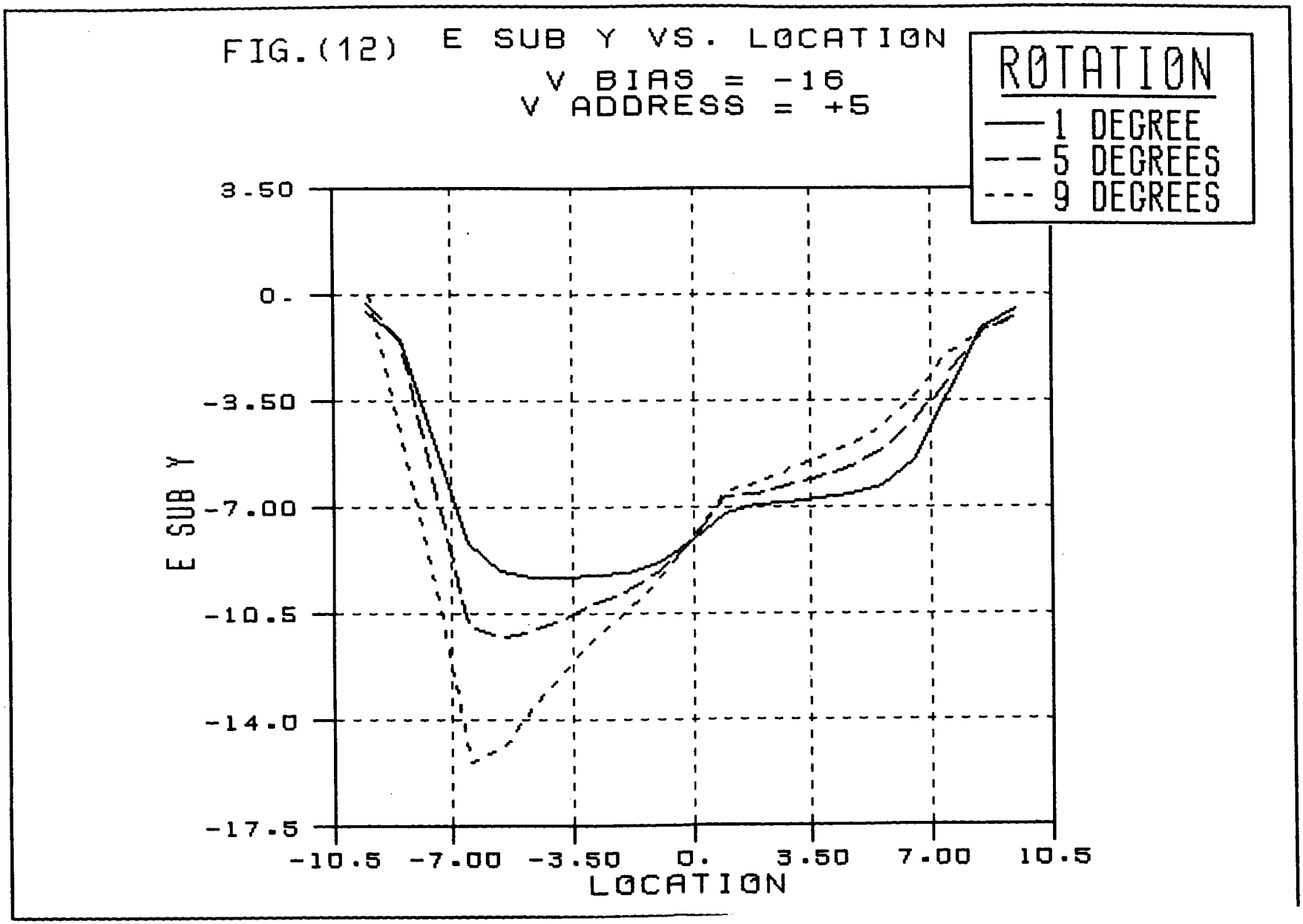
FIG.(12) E SUB Y VS. LOCATION
V BIAS = -16
V ADDRESS = +5
ROTATION
1 DEGREE
5 DEGREES
9 DEGREES
3.50
0.
-3.50
-7.00
-10.5
-14.0
-17.5
E SUB Y
-10.5
-7.00
-3.50
0.
3.50
7.00
10.5
LOCATION

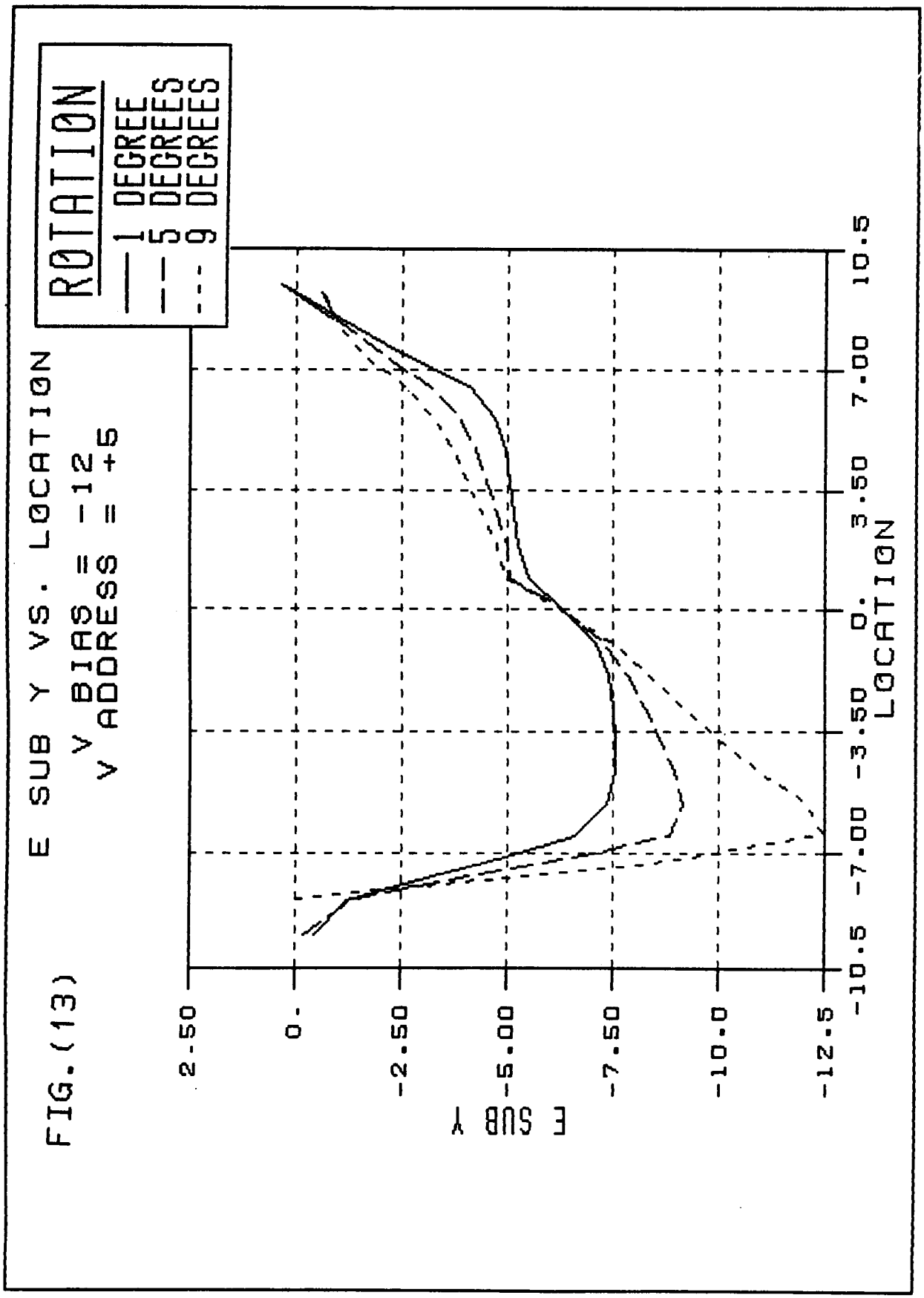
E SUB Y VS. LOCATION
V BIAS = -12
V ADDRESS = +5
ROTATION
1 DEGREE
5 DEGREES
9 DEGREES
E SUB Y
2.50
0.
-2.50
-5.00
-7.50
-10.0
-12.5
-10.5
-7.00
-3.50
0.
3.50
7.00
10.5
LOCATION

FIG.(13)

FIG.(14): DMD VIBRATION MODES

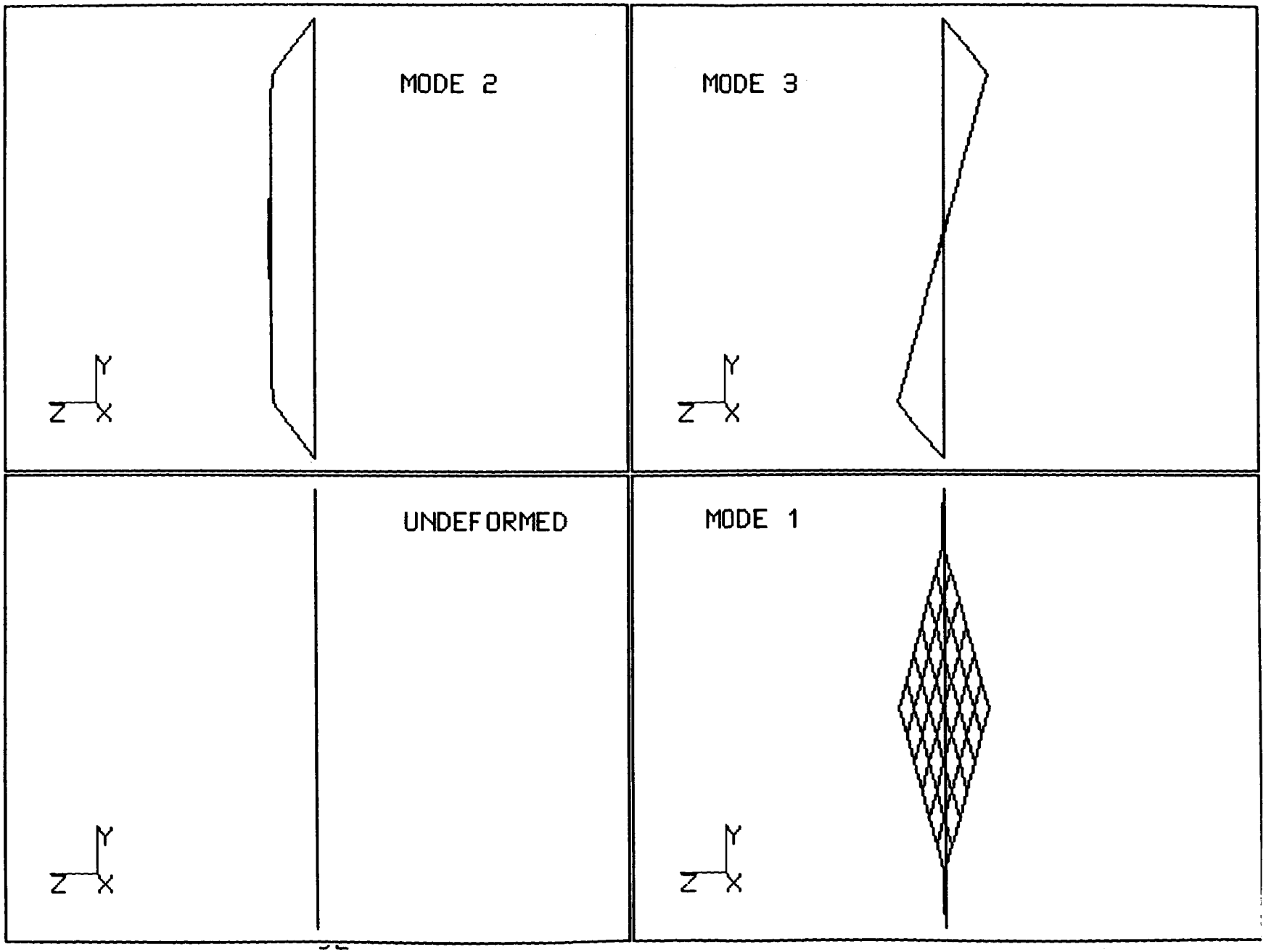

FIG. (15)

BISTABLE DMD

DIFFERENTIAL BIAS VS ADDRESS VOLTAGE

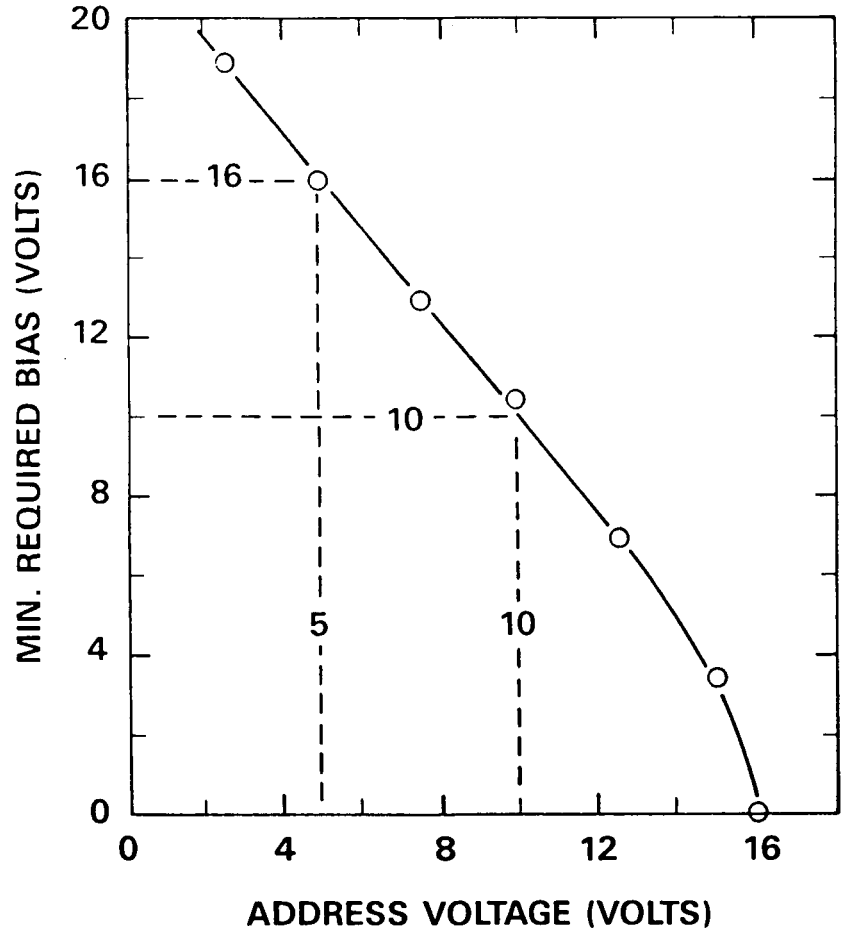

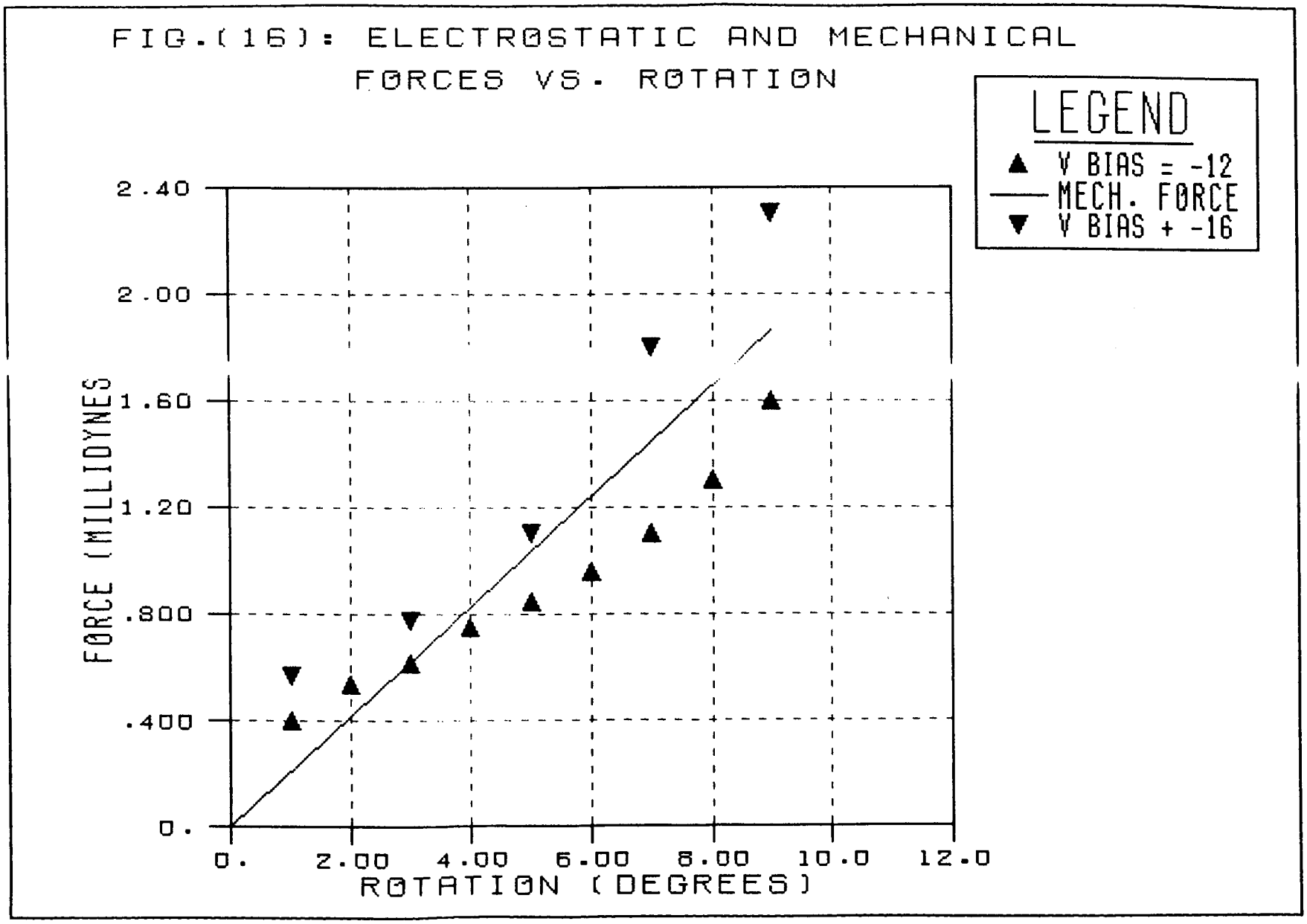
FIG.(16): ELECTROSTATIC AND MECHANICAL FORCES VS. ROTATION
LEGEND
V BIAS = -12
MECH. FORCE
V BIAS + -16
2.40
2.00
1.60
1.20
.800
.400
0.
FORCE (MILLIDYNES)
0.
2.00
4.00
6.00
8.00
10.0
12.0
ROTATION (DEGREES)